Materials Chemistry and Physics 125 (2011) 174–183

Contents lists available at ScienceDirect

Materials Chemistry and Physics

journal homepage: www.elsevier.com/locate/matchemphys

Morphology and thermal properties of organic–inorganic hybrid material involving monofunctional-anhydride POSS and epoxy resin

Yiting Xu, Yingying Ma, Yuanming Deng, Cangjie Yang, Jiangfeng Chen, Lizong Dai*

Department of Material Science and Engineering, College of Materials, Xiamen University, No. 422, Siming South Road, 361005 Xiamen, Fujian Province, China

ARTICLE INFO

Article history:
Received 4 February 2010
Received in revised form 9 July 2010
Accepted 1 September 2010

Keywords:
Monofunctional-anhydride POSS
Epoxy resin
Morphology
Thermal properties

ABSTRACT

Monofunctional-anhydride polyhedral oligomeric silsesquioxane ($i\text{-}C_4H_9)_7Si_8O_{12}OSi(CH_3)_2(C_8H_9O_3$) (AH-POSS) was synthesized and characterized by FTIR, NMR, element analysis. Then AH-POSS was incorporated into epoxy system either pre-reacted or non-reacted using hexahydrophthalic anhydride (HHPA) as curing agent. Pre-reacted system hybrid materials were obtained by two-step preparation. First, AH-POSS reacted with part of diglycidyl ether of bisphenol A (DGEBA) to form AH-POSS-epoxy precursor in DGEBA, then cured with HHPA. Non-reacted POSS/epoxy hybrid materials were prepared by directly mixing AH-POSS, HHPA and DGEBA together and cured afterwards. The GPC and FTIR spectra suggested successful bonding of AH-POSS and epoxy resin. Morphologies of hybrid materials were characterized by SEM and TEM. Non-reacted system led to a dispersion of spherical particles with sizes in the range of micrometers. For pre-reacted system, polymerization-induced phase separation took place with POSS content lower than 30 wt% and also some "vesicle" structure was formed after curing. A typical macro-phase separation happened with POSS content up to 40 wt% before and after curing. The glass transition temperatures (T_g's) and the storage modulus were measured by dynamic mechanical analysis (DMA). T_g's and modulus displayed irregularly decrease. The initial thermal decomposition temperatures (T_d's) characterized by TGA were also irregularly decreasing for both systems. However, they were higher than those of epoxy composites when using amine as the curing agent.

1. Introduction

Polyhedral oligomeric silsesquioxanes (POSS) are nanosized cage structures with some organic R groups, and are one of the most useful siloxane. POSS can be incorporated into polymers to build organic–inorganic hybrid materials [1–4]. Some of the organic functional substituent groups are reactive and are the main factor to decide the compatibility with polymer matrix [5–10]. POSS could be incorporated into polymers via blending, copolymerization or some other chemical approaches. During the past years, sorts of POSS monomers have been incorporated into thermosetting polymer to prepare the nanocomposites with different thermomechanical properties and morphologies [11–16].

Nowadays, epoxy resin become one of the most popular commercial resin, and POSS/epoxy hybrid materials are attracted more and more attention among POSS/polymer hybrid materials [17–19]. The incorporation of POSS into the epoxy resin offers the opportunity to enhance the physical properties for advanced electronic, aerospace and automotive applications [20,21]. During the past years, a lot of researches have been done. Williams et al. [22] observed that a primary phase separation appeared at the time of adding the POSS-diamine precursors to epoxy because of the incompatibility between epoxy and POSS. It is noted that the nature of the organic inert groups and pre-reaction of a monofunctional POSS have pronounced impact on the morphology. Zheng et al. [21] reported that the different morphological structures could be formed in the POSS-containing hybrid composites depending on the types of R groups. Matejka et al. [23] investigated that the structure and properties of epoxy networks improved with POSS, and the effects of POSS–POSS interactions on the thermal properties were addressed. Most of the nanocomposites showed relatively low T_g's in comparison with the control epoxy [24]. A new octa(2,3-epoxypropyl)-silsesquioxane (OE) was prepared by Lee and Chen [8]. The thermosetting composites containing OE exhibited a high T_g of 170 °C. Lee and Lichtenhan [11] also found that macro-phase separation was observed in the hybrid materials because of the presence of inert aliphatic groups in the residual arms of POSS with the POSS content higher than 10%. Liu's approach [25] was based on Williams' in order to obtain homogeneous epoxy/POSS hybrid materials containing large mass fractions of POSS. Amine-POSS first reacted with part of epoxy chain to give an amine-POSS-epoxy pre-

* Corresponding author. Tel.: +86 592 2186178; fax: +86 592 2183937.
E-mail address: lzdai@xmu.edu.cn (L. Dai).

0254-0584/$ – see front matter © 2010 Elsevier B.V. All rights reserved.
doi:10.1016/j.matchemphys.2010.09.003

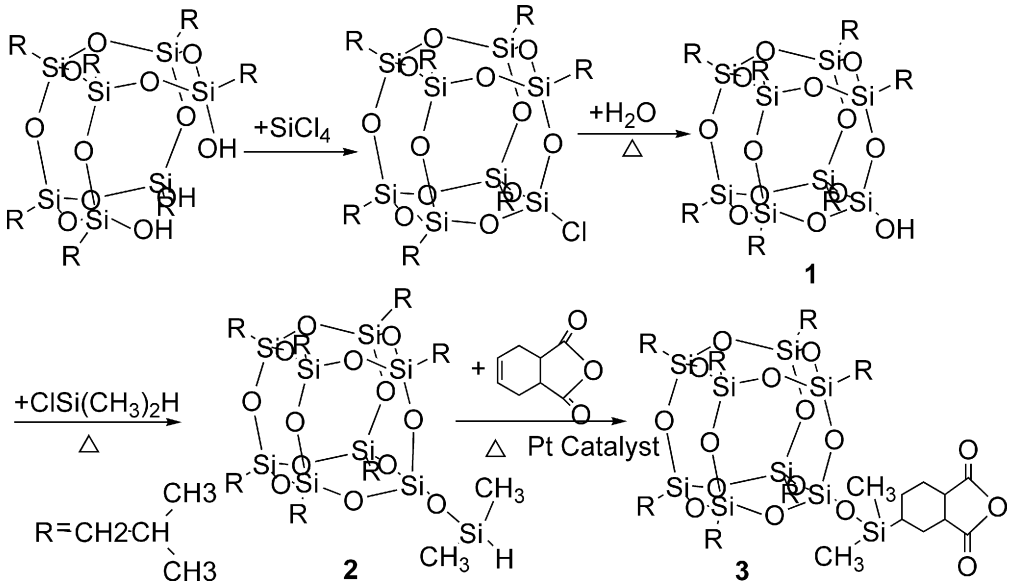

Scheme 1. Synthesis of AH-POSS.

cursor and then cured. POSS content in the hybrid material was about 50 wt%.

All of the previous studies reported the modification of epoxy thermosets using POSS via the chemical reaction between polymer matrix and POSS. In our work (Scheme 1), we designed and synthesized monofunctional-anhydride POSS (i-$C_4H_9)_7Si_8O_{12}OSi(CH_3)_2(C_8H_9O_3)$ (AH-POSS), which could be incorporated into epoxy to prepare the organic–inorganic hybrid material based on Liu's approach [25]. To the best of our knowledge, there has been no precedent report on the hybrid materials of epoxy with a large mass fraction of AH-POSS with anhydride as curing agent. Meanwhile, there has also been no report about the mechanical properties of hybrid materials with a large mass fraction of AH-POSS with curing agent HHPA. Pre-reacted system was designed that AH-POSS-epoxy precursor was synthesized through the reaction between DGEBA and AH-POSS (Scheme 2). The system was then cured to generate an AH-POSS/epoxy hybrid material with HHPA as curing agent. For comparison, non-reacted system was also obtained through directly mixing DGEBA, AH-POSS, HHPA and then cured. The morphologies of the two types of inorganic–organic hybrid materials were comparatively investigated on the basis of scanning electronic microscopy (SEM), transmission electronic microscopy (TEM). The glass transition temperatures (T_g's) and modulus (E's) were measured by dynamic mechanical thermal analysis (DMTA) and initial decomposition temperatures (T_d's) were measured by thermogravimetric analysis (TGA). Some advantages with anhydride as curing agent were found such as less poisonous and better thermal stability than those epoxy cured with amine curing agent.

2. Experimental

2.1. Materials

TriSilanolIsobutyl POSS ((i-$C_4H_9)_7Si_8O_9(OH)_3$) was purchased from Hybrid Plastics Co. Tetrachlorosilane ($SiCl_4$), chlorodimethylsilane ($Cl(CH_3)_2SiH$), cis-1,2,3,6-tetrahydrophthalic anhydride (THPA), hexahydrophthalic anhydride (HHPA) and Karstedt's catalyst were purchased from Alfa Aesar and used as received. Diglycidyl ether of bisphenol A (DGEBA) (Epon 828, epoxy equivalent weight 188.05 g mol^{-1}) was received from Shell Co. Ltd. A tertiary amine catalyst 1-cyanoethyl-2-undecylimidazole ($C_{11}Z$–CN) was purchased from Guangzhou Huangpu W-union Chemical Co. Ltd. Unless specially indicated, other reagents such as sodium, calcium hydride (CaH_2), tetrahydrofuran (THF), triethylamine (Et_3N), acetonitrile (CH_3CN), toluene, *n*-hexane and acetone were of analytical pure grade, purchased from Shanghai Reagent Company of China. Before use, THF was refluxed above sodium, distilled and then stored in the presence of the molecular sieve of 4 Å. Triethylamine and toluene were refluxed over CaH_2 and filtered, then stored in the presence of the molecular sieve of 4 Å and KOH.

2.2. Synthesis of [(i-$C_4H_9)_7Si_8O_{12}(OH)$]

Under a dry nitrogen atmosphere, $SiCl_4$ (1.700 g, 10 mmol) was added to a solution of (i-$C_4H_9)_7Si_8O_9(OH)_3$ (7.910 g, 10 mmol) and Et_3N (3.036 g, 10 mmol) in THF (50 mL). The mixture was stirred overnight and then filtered to remove Et_3NHCl. Evaporation of the volatiles gave crude product (i-$C_4H_9)_7Si_8O_{12}Cl$ (7.981 g), yield 95.8%. Large colorless crystals of (i-$C_4H_9)_7Si_8O_{12}Cl$ (6.658 g), yield 80%, were obtained by recrystallization in CH_3CN and saturated toluene. Then the suspension of (i-$C_4H_9)_7Si_8O_{12}Cl$ (6.658 g, 8.00 mmol) in THF/H_2O (2:1, 50 mL) was refluxed for 70 h. Evaporation of the volatiles afforded crude product 1 as white solid. Subsequently, recrystallization from a hot toluene/acetonitrile mixture and dried in vacuum to gave pure product 1 6.500 g, yield 97.6% [26]. ^1H NMR (400 MHz, $CDCl_3$, 25 °C, ppm): 0.62 (d, 14H), 0.96 (d, 42H), 1.85 (m, 7H), 2.49 (broad, 1H). ^{13}C NMR (400 MHz, $CDCl_3$, 25 °C, ppm): 22.26, 22.38, 22.45 (–CH_2, 1:3:3), 23.78, 23.83 (–CH), 25.64, 25.66 (–CH_3). ^{29}Si NMR (300 MHz, 25 °C, ppm): −65.67, −65.82 (3:4), −101.02 (Si–OH). Anal. calcd for ($iC_4H_9)_7Si_8O_{12}(OH)$: C, 40.38; H, 7.69. Found: C, 40.78; H, 7.97.

2.3. Synthesis of [(i-$C_4H_9)_7Si_8O_{12}OSi(CH_3)_2H$]

Under a dry nitrogen atmosphere, the solution of $ClSi(CH_3)_2H$ (0.738 g, 7.8 mmol) in THF (5 mL) was added to the solution of (i-$C_4H_9)_7Si_8O_{12}(OH)$ (6.500 g, 7.8 mmol) and Et_3N (2.363 g, 23.4 mmol, 3 equiv) in THF (50 mL) contained in a thick-walled glass reactor. A precipitate of Et_3NHCl formed upon addition of the chlorosilane. The reaction mixture was heated at 60 °C for 18 h. Then the reaction mixture was transferred to a separatory funnel. The reaction vessel was rinsed with diethyl ether and the ether washings were combined with THF. The THF/ether phase was washed with successive portions of H_2O (50 mL), 1 mol L^{-1} HCl (50 mL), H_2O (50 mL), and saturated NaCl (50 mL). The THF/ether phase was dried over $MgSO_4$, filtered, and THF/ether was removed under vacuum to give 6.751 g of (i-$C_4H_9)_7Si_8O_{12}O(CH_3)_2H$ as white powder, yield 97% [27]. ^1H NMR (400 MHz, $CDCl_3$, 25 °C, ppm): 0.22 (d, J = 2.78, 6H), 0.61 (d, 14H), 0.96 (d, 42H), 1.85 (m, 7H), 4.71 (sept, J = 2.78 Hz, 1H). ^{13}C NMR (400 MHz, $CDCl_3$, 25 °C, ppm): 0.176 (Si–CH_3), 22.33, 22.42, 22.48 (isobutyl-CH_2, 1:3:3), 23.80, 23.85 (isobutyl-CH), 25.67, 25.68 (isobutyl-CH_3). ^{29}Si NMR (300 MHz, 25 °C, ppm): −4.108 (–$OSi(CH_3)_2H$), −67.172, −67.979 (3:4, isobutyl-Si), −109.791 (–$SiOSi(CH_3)_2$). FTIR (KBr, thin film, cm^{-1}): 2139 (Si–H), 1119 (Si–O–Si). Anal. calcd for (i-$C_4H_9)_7Si_8O_{12}O(CH_3)_2H$: C, 40.41; H, 7.91; Found: C, 40.30; H, 8.31.

2.4. Synthesis of AH-POSS [(i-$C_4H_9)_7Si_8O_{12}OSi(CH_3)_2(C_8H_9O_3)$]

(i-$C_4H_9)_7Si_8O_{12}OSi(CH_3)_2(C_8H_9O_3)$ was prepared by hydrosilylation reaction of (i-$C_4H_9)_7Si_8O_{12}OSi(CH_3)_2H$ with THPA under a dry argon atmosphere. In a 20 mL two-necked round-bottomed flask equipped with a magnetic stirrer,

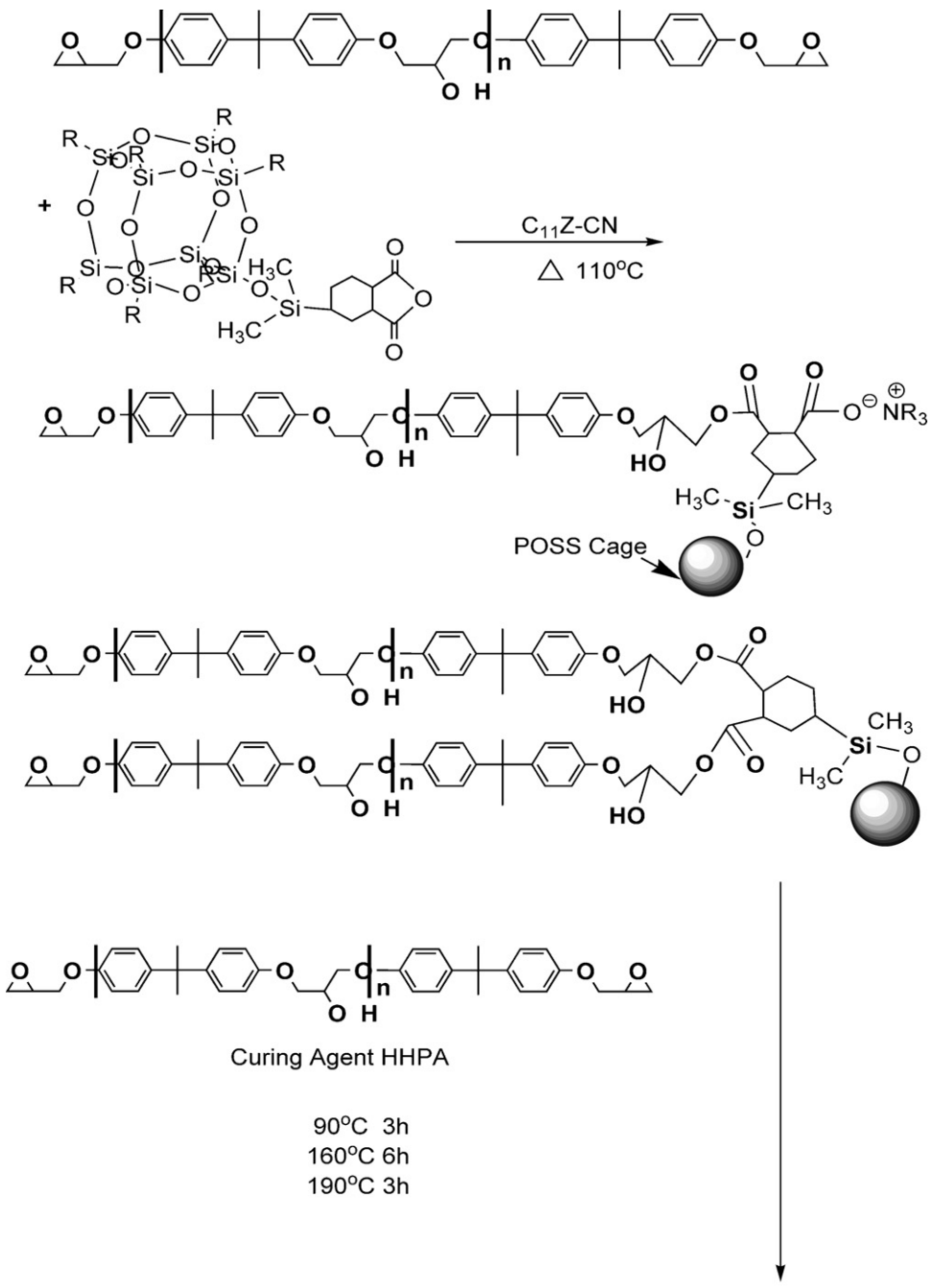

Scheme 2. Preparation for AH-POSS-epoxy precursor and the hybrid material.

$(i\text{-}C_4H_9)_7Si_8O_{12}OSi(CH_3)_2H$ (6.751 g, 7.58 mmol), THPA (1.156 g, 7.60 mmol) and toluene 20 mL were placed under an argon stream. The reaction was carried out with Karstedt's catalyst (Pt(dvs)) (0.61 mmol) in toluene at 55 °C for 48 h [28]. After solvent removal, the solid was refluxed in hexane for 30 min and the mixture was filtered to remove residual THPA. The Pt catalyst was extracted from the solid by refluxing in acetone with active carbon for several hours and the precipitate was filtered and washed with acetone. Finally, the solid was refluxed in acetic anhydride and toluene for 2 h, followed by solvent removal, and then dried at 180 °C to afford $(i\text{-}C_4H_9)_7Si_8O_{12}OSi(CH_3)_2(C_8H_9O_3)$ 7.114 g, yield 90%. ^{1}H NMR (400 MHz, $CDCl_3$, 25 °C, ppm): 0.18 (d, 6H), 0.61 (t, 14H), 0.85 (m, 1H), 0.96 (d, 42H), 1.85 (m, 13H), 2.37 (m, 2H). ^{13}C NMR (400 MHz, $CDCl_3$, 25 °C, ppm): 1.01 (Si–CH_3), 20.84, 20.05, 22.42 and 22.35 (4:3, Si-isobutyl CH_2), 21.91 (–O–Si(CH_3)$_2$–CH–), 23.28, 23.84, 25.69, 39.71, 41.50, 170.90, 172.97. ^{29}Si NMR (300 MHz, 25 °C, ppm): −110.75 (–SiOSi(CH_3)$_2$), −67.17, −67.98 (3:4, isobutyl-Si), −11.02 (–OSi(CH_3)$_2$). FTIR (KBr, thin film, cm^{-1}): 1727, 1789 and 1885 (anhydride), 1120 (Si–O–Si). Anal. calcd for $(i\text{-}C_4H_9)_7Si8O_{12}OSi(CH_3)_2(C_8H_9O_3)$: C, 43.73; H, 7.53. Found: C, 43.36; H, 7.19.

2.5. Preparation of pre-reacted system hybrid material

The desirable amount of AH-POSS was mixed with DGEBA using C_{11}Z–CN as catalyst in toluene through continuous stirring at 110 °C for 3 h until the homogeneous and light yellow mixture was obtained. Then toluene was evaporated with a rotary evaporator. Desirable amount of HHPA and C_{11}Z–CN were added into the system with vigorous stirring. The mixtures were degassed in a vacuum oven for 3 h at 50 °C and poured into an aluminum foil. The mixture was cured at 90 °C for 3 h and 160 °C for 6 h plus 190 °C for 3 h. The pre-reacted system organic–inorganic POSS/epoxy hybrid materials were prepared with the content of AH-POSS up to 40 wt% of the pure DGEBA.

2.6. Preparation of non-reacted system hybrid material

Desirable amount of AH-POSS, DGEBA and HHPA were mixed in toluene (1 mL) through continuous stirring at 110 °C for 50 min until the homogeneous mixture was obtained. Then toluene was evaporated with a rotary evaporator. After that, desirable amount of $C_{11}Z$–CN as catalyst was added into the system through vigorous stirring. The mixture was degassed in a vacuum oven for 3 h at 50 °C and poured into an aluminum foil. The mixture was cured at 90 °C for 3 h and 160 °C for 6 h plus 190 °C for 3 h. The non-reacted system POSS/epoxy hybrid materials were prepared with the content of AH-POSS up to 5 wt% of the pure DGEBA. However, when AH-POSS content was higher than 5 wt%, the samples were easily splitted and could not be used for testing. So the amount of AH-POSS has been only added up to 5 wt% of pure DGEBA.

2.7. Characterization

2.7.1. Nuclear magnetic resonance spectroscopy (NMR)

^1H and ^{13}C NMR measurements were carried out on a Bruker AV400 MHz NMR spectrometer. ^{29}Si NMR measurement was carried on a Bruker AV300 MHz. For ^1H NMR and ^{13}C NMR measurements, the samples were dissolved with d-chloroform and the solutions were measured with tetramethylsilane (TMS) as the internal reference. The high-resolution solid-state ^{29}Si NMR spectra were obtained using cross polarization (CP)/magic angle spinning (MAS) together with the high-power dipolar decoupling (DD) technique. The rate of MAS was 5.0 kHz for measuring the spectra.

2.7.2. Fourier transform infrared spectroscopy (FTIR)

FTIR measurements were conducted on an AVATAR 360 FTIR (Nicolet Instrument) at room temperature (25 °C). The sample was prepared by mixing the polymer with KBr and then pressed into small flakes. In all cases, 32 scans at a resolution of 4 cm^{-1} were used to record the spectra.

2.7.3. Transmission electronic microscopy (TEM)

TEM was performed on a JEM 2100 high-resolution transmission electron microscope at the accelerating voltage of 200 kV. The samples were trimmed using an ultramicrotome, and the specimen sections (90–100 nm in thickness) were placed in 200 mesh copper grids for observation.

2.7.4. Scanning electron microscopy (SEM)

In order to observe the morphological structures, the thermosets were fractured under cryogenic condition using liquid nitrogen. Then all the samples were etched by CH_2Cl_2 for 30 min. The etched specimens were dried to remove the solvents. The fracture surfaces were coated with thin layers of gold of about 100 Å. The thermosets were observed by means of a XL-30 Environmental Scanning Electron Microscope at an activation voltage of 20 kV.

2.7.5. Thermogravimetric analysis (TGA)

Simultaneous Thermal Analysis (NETZSCH STA 409EP) was used to investigate the thermal stability of the hybrid material. All of the thermal analyses were conducted in nitrogen atmosphere from ambient temperature to 900 °C at the heating rate of 10 °C min^{-1}. The thermal degradation temperature was taken as the onset temperature at which 5 wt% of weight loss occurs.

2.7.6. Dynamic mechanical thermal analysis (DMTA)

The dynamic mechanical tests were carried out on a Dynamic Mechanical Thermal Analyzer (DMTA) (MKIV, Rheometric Scientific Inc., USA) with the temperature ranging from 30 to 180 °C. The frequency used is 1.0 Hz at the heating rate 3.0 °C min^{-1}. The specimen dimension was 3 cm × 1 cm × 0.2 cm.

2.7.7. Gel penetration chromatography (GPC)

GPC was measured with Aliglent 1100LC GPC instrument (set at 30 °C) equipped ISO water pump. The eluent was THF at a flow rate of 1.0 mL min^{-1}. Elution time was 23 min. A series of low polydispersity polystyrene standards were employed for the GPC calibration.

3. Results and discussion

3.1. Characterization of AH-POSS $[(i\text{-}C_4H_9)_7Si_8O_{12}OSi(CH_3)_2(C_8H_9O_3)]$

The synthesis route for $(i\text{-}C_4H_9)_7Si_8O_{12}OSi(CH_3)_2(C_8H_9O_3)$ was described in Scheme 1. First, $(i\text{-}C_4H_9)_7Si_8O_{12}OSi(CH_3)_2H$ was prepared by the methods reported by Shockey et al. [27]. FTIR, ^{29}Si NMR and ^{13}C NMR spectra (Figs. S1, S2 and S3 in supporting information) can indicate that the cubic silsesquioxane and the POSS with $–O–Si(CH_3)_2H$ group was successfully obtained.

AH-POSS was prepared via the reaction between $(i\text{-}C_4H_9)_7Si_8O_{12}OSi(CH_3)_2H$ and THPA in presence of Karstedt's catalyst. In order to promote the complete conversion of hydrosilylation, slightly excessive THPA was used and the reaction time was 48 h. According to the difference in solubility, excessive THPA was easily isolated from the reacted mixtures through filtrating from hexane solution. According to the peaks in ^{13}C NMR and ^{29}Si NMR (Figs. S4 and S5 in supporting information), it could be inferred that AH-POSS was successfully prepared. And the result of elemental analysis for the product in each step agrees well with theoretical value by calculation (Table 1).

Table 1
Elemental analysis data of the product in each step of AH-POSS preparation procedure.

Compound		Element	
		C	H
$(i\text{-}C_4H_9)_7Si_8O_{12}(OH)$	Theo. (%)	40.38	7.69
	Exp. (%)	41.54	7.97
$(i\text{-}C_4H_9)_7Si_8O_{12}OSi(CH_3)_2H$	Theo. (%)	40.41	7.91
	Exp. (%)	40.30	8.31
$(i\text{-}C_4H_9)_7Si_8O_{12}OSi(CH_3)_2(C_8H_9O_3)$	Theo. (%)	43.73	7.53
	Exp. (%)	43.16	7.12

3.2. Synthesis of POSS-epoxy precursor in pre-reacted system

The organic–inorganic AH-POSS was incorporated into DGEBA to form AH-POSS-epoxy precursors (Scheme 2).

First, AH-POSS, which could react with DGEBA resulting in AH-POSS-epoxy precursor, was used in this work. The reaction between AH-POSS and DGEBA was evidenced by FTIR (Fig. 1) and GPC (Fig. 2). The appearance of the new absorption peak at 1736 cm^{-1} and the slight movement of the peak at 3420–3500 cm^{-1} indicate that the ring-open addition reaction occurs between AH-POSS and DGEBA. The absorption of the peak 1108 cm^{-1} is assignable to the stretching vibration of Si–O–Si bond.

The result of pre-reaction between AH-POSS and DGEBA was also confirmed by GPC. There are two shifts, indicating the formation of higher molecular mass unites, could be observed in Fig. 2. The larger molecules, that AH-POSS bonded one or two DGEBA chains shown as Scheme 2, is obviously formed. GPC analysis of AH-POSS-epoxy precursor provides additional support for the aforementioned [25]. AH-POSS-epoxy precursor can be directly mixed with DGEBA and cured under conventional conditions.

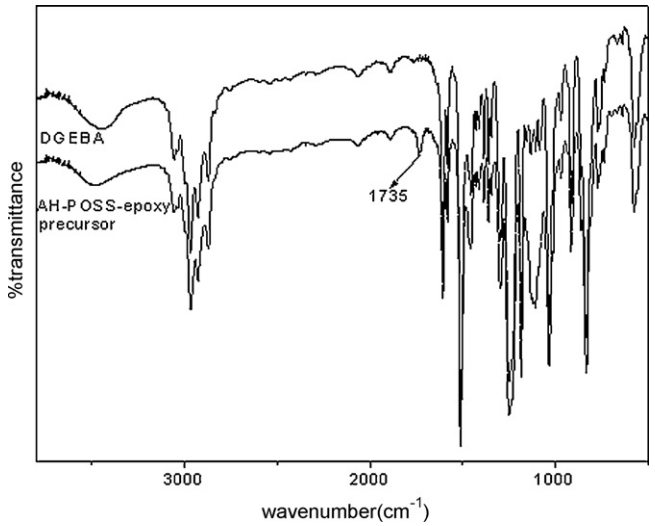

Fig. 1. FTIR spectra of DGEBA and AH-POSS-epoxy precursor.

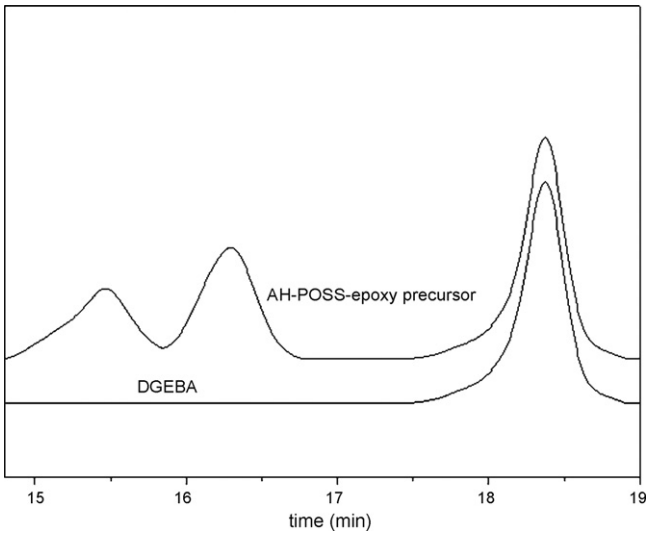

Fig. 2. GPC chromatograms of DGEBA Epon 828 and AH-POSS-epoxy precursor.

3.3. Morphology of hybrid material

Before curing, the mixtures with AH-POSS content lower than 30 wt% were homogeneous and transparent in pre-reacted system, which suggested that no macro-phase separation happened at the scale exceeding the visible wavelength. But the mixture with higher AH-POSS content up to 40 wt% was ivory-white, which means that macro-phase separation occurred. It is plausibly proposed that the DGEBA has a certain capacity of solubility of AH-POSS-epoxy precursor. After curing, the samples changed gradually from clarity to opaque with lower AH-POSS content (Table 2), which suggested that the polymerization-induced phase separation occurred when POSS content was lower than 30 wt%. The morphologies of the hybrid materials were examined by means of SEM and TEM.

Table 2
The comparison of the change of pre-reacted system before and after curing.

AH-POSS (wt%)	Before curing	After curing
0	Clarity	Clarity
5	Clarity	Clarity
10	Clarity	Clarity
20	Clarity	Opaque
30	Clarity	Opaque
40	Ivory-white	Opaque

The use of low molecular weight curing agents in the preparation of hybrid materials makes a kind of dispersion more facile [22,29]. Some irregular clusters in sizes about 0.2 to 2 μm could be observed in SEM (Fig. 3). The clusters were considered as the POSS-rich domains. Separated smooth (epoxy-rich region) and rough (POSS-rich region) macro-domains were observed with higher AH-POSS content [25]. The samples were etched with dichloromethane before SEM analysis. It is easily seen that the irregular clusters could not be soluble by dichloromethane, which indicates that the irregular clusters have already taken part in the formation of epoxy network. And the POSS domains might form during polymerization-induced phase separation process with AH-POSS content lower than 30 wt%. For pre-reacted system, a magnification picture of one of these clusters is shown in Fig. 4. There are some irregular clusters that can be pulled out from the epoxy matrix on the section.

The ultrathin sections of the organic–inorganic hybrid materials were subjected to TEM (Fig. 5). In term of the difference in atomic number contrast between organic and inorganic portion (viz., POSS moiety), the dark area is assignable to POSS portion. It could be seen that AH-POSS-epoxy precursors dispersed in the continuous epoxy matrix with the average size of approximately 0.2–2 μm. The results are constituent with that of the analysis of SEM figures. It is proposed the formation of the irregular clusters could be explained by the interaction of POSS–POSS and the mechanism of polymerization inducing phase separation [21]. This phase separa-

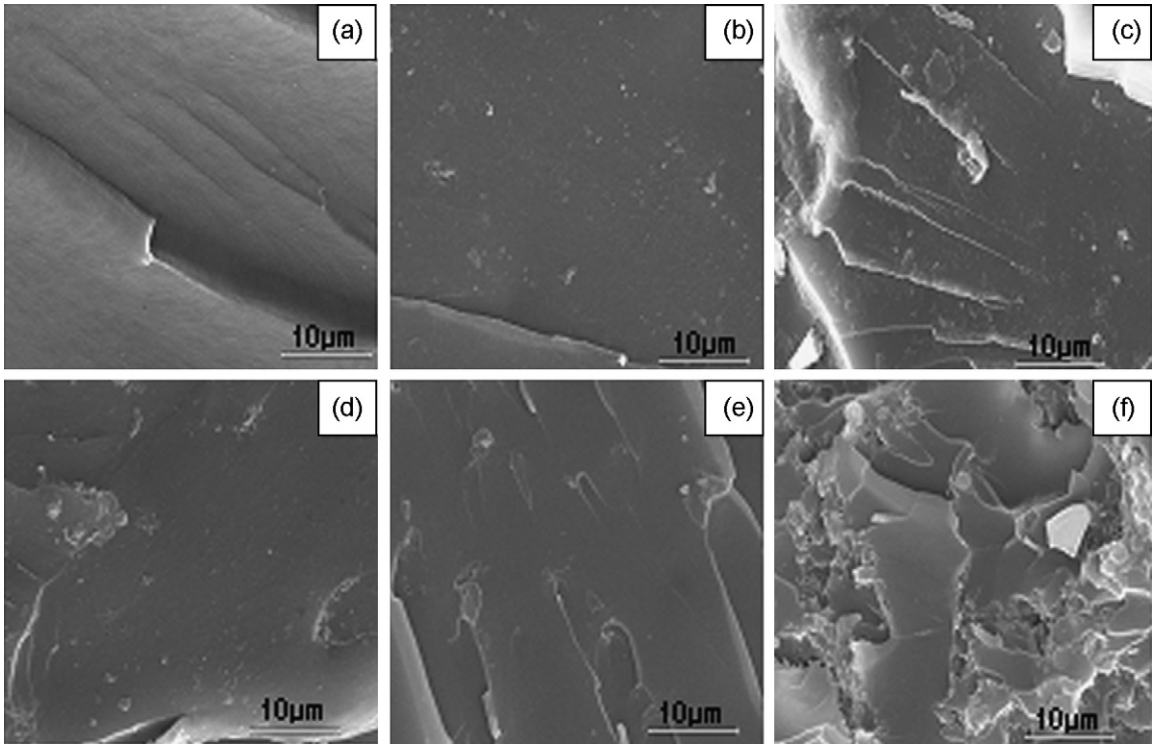

Fig. 3. SEM micrograph of the sections of pre-reacted hybrid materials with different AH-POSS contents (wt%): (a) 0; (b) 5; (c) 10; (d) 20; (e) 30 and (f) 40.

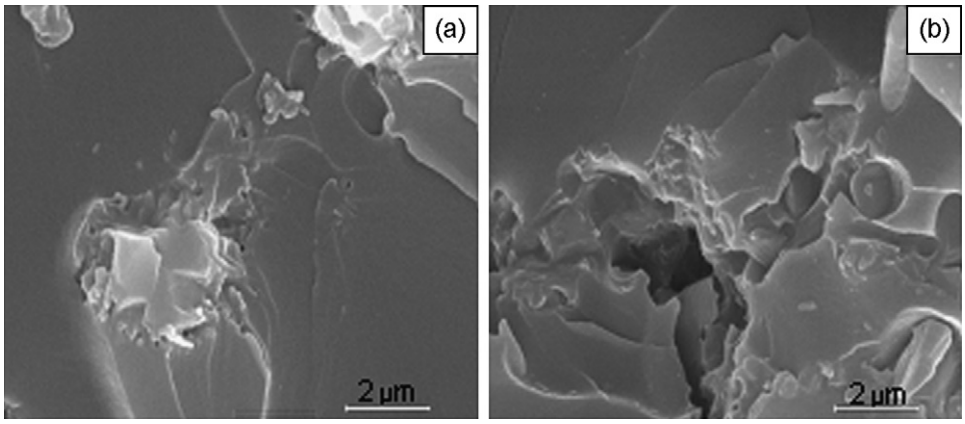

Fig. 4. SEM micrograph of the sections of pre-reacted hybrid materials with 30 wt% AH-POSS containing irregular clusters (a) and cavities (b).

tion occurred when mixing DGEBA and AH-POSS-epoxy precursor due to the incompatibility between the isobutyl groups of the POSS molecules and the aromatic epoxy. Additionally, POSS molecules with cagelike nanostructure tend to form random aggregations to reduce interfacial energy.

It is plausibly proposed that DGEBA is a kind of selective solvent for AH-POSS-epoxy precursor. In fact, AH-POSS monomer is incompatible with DGEBA. When the AH-POSS content is lower than 30 wt%, the AH-POSS-epoxy precursor is easily soluble in DGEBA before curing. After curing, some POSS aggregates, which is called irregular clusters, are formed because of the incompatibility of isobutyl and epoxy matrix and the interaction of POSS–POSS. Meanwhile, some "vesicle" areas are also formed in the cluster. The "vesicle" structures were further fixed with the magnification of TEM figure (Fig. 5c) and depicted in Scheme 3. It is seen that the irregular clusters consist of small domains with the diameter of about 20 nm (Fig. 5b and Scheme 3). The domain is presented as "vesicle" structure. The results of magnification figure of TEM (Fig. 5c and Scheme 3) indicate that there are also some epoxy chains inside of the domains, which form the core of "vesicle". And POSS aggregates together to form the shell of "vesicle" because of the interaction of the isobutyl groups and parts of epoxy chains are enwrapped. Depending on the miscibility of AH-POSS-epoxy precursor and the epoxy matrix, the formation of "vesicle" structure could be accounted for polymerization-induced phase separation mechanisms.

The significant differences between the two systems for both formulations are also reflected in Fig. 6. For non-reacted system, there are some spherical holes dispersed non-uniformly and sparsely in the DGEBA matrix with sizes of about 1–2 μm, which are the residual AH-POSS extracted by CH_2Cl_2. With the increase of AH-POSS content, it almost keeps unchanged in the size of spherical holes, but becomes more in number. Because of the incompatibility between AH-POSS and DGEBA, the AH-POSS aggregates together before curing and the parts of AH-POSS could not take part in the cure reaction. Obviously there are also a few irregular clusters, which could not be soluble in CH_2Cl_2. It could be assumed that perhaps some AH-POSS reacted with DGEBA during the curing process. The morphologies of the irregular clusters also look like those in pre-reacted system.

3.4. Thermal properties

3.4.1. Glass transitions behavior

The glass transition behavior was confirmed by DMTA (Fig. 7). The control epoxy exhibited a well-defined relaxation transition centered at 131.0 °C which is attributed to the glass transition of the epoxy thermoset. For pre-reacted system hybrid materials, the DMTA thermograms display single T_g in the test temperature range (30–180 °C). Compared to the T_g's of control epoxy, the T_g's of hybrid materials are irregularly decreasing with the increase of AH-POSS content.

The degree of curing reaction will mainly affect the T_g's and E's of the hybrid materials. So FTIR was used to examine the degree of curing reaction for both systems (shown in Fig. 8). The pure DGEBA is characterized by the stretching vibration band of epoxide groups at 915 cm^{-1} and all the epoxide bands disappeared after curing for both systems. Meanwhile, the band of 1731 cm^{-1} appeared and the carbonyl groups were formed. It could be considered that curing reactions have been carried out to completion. Therefore,

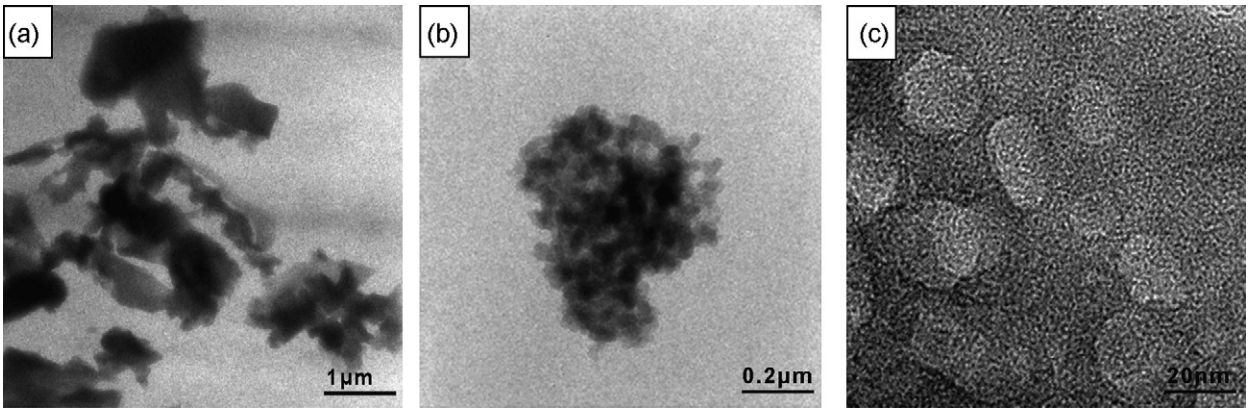

Fig. 5. TEM micrograph of pre-reacted system hybrid materials containing 20 wt% AH-POSS with different magnifications.

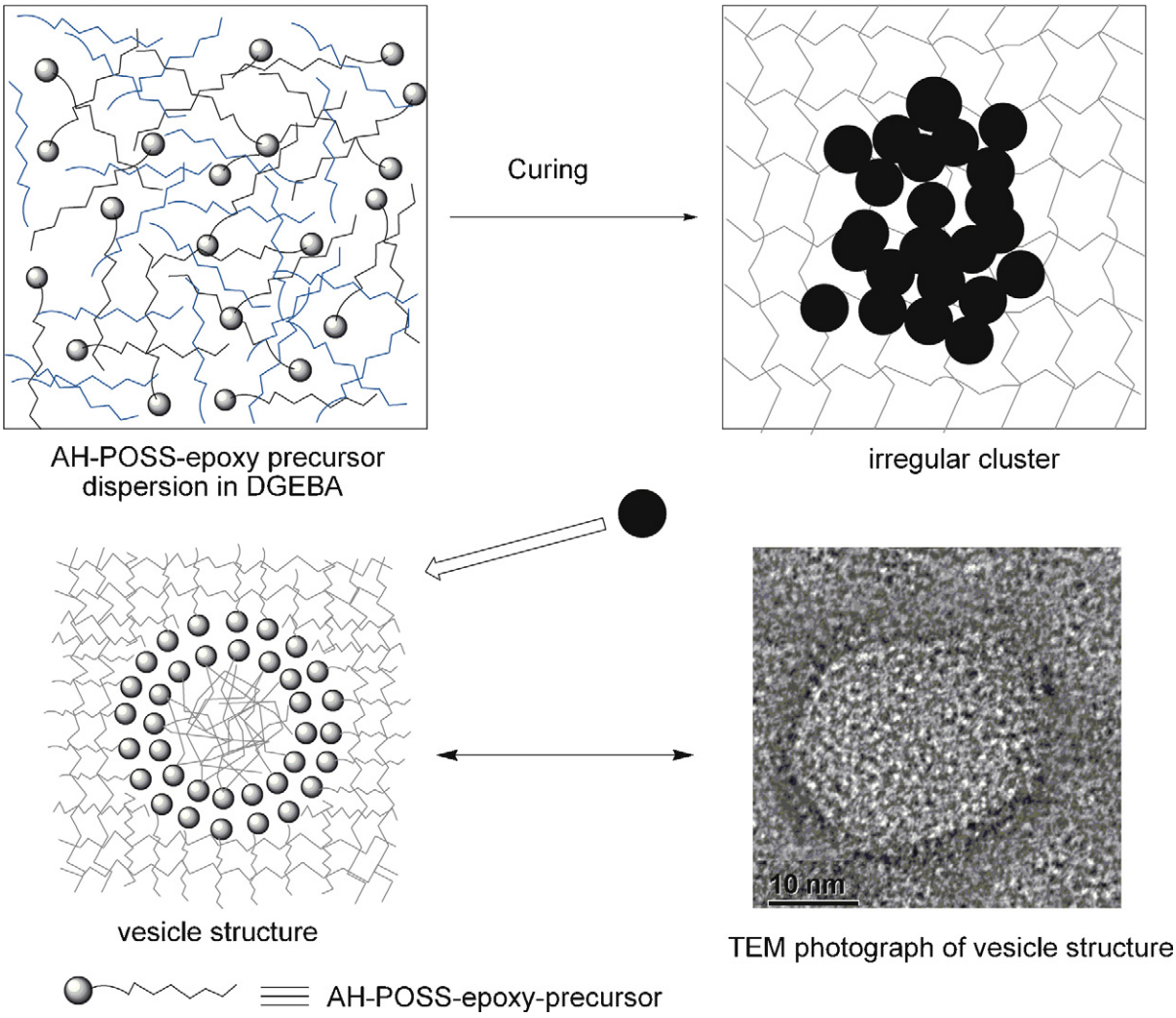

Scheme 3. The simulated diagram of formation of inside "vesicle" structure in pre-reacted system hybrid material.

the depression of T_g's could be ascribed to other reason for both systems.

For pre-reacted system hybrid materials, it has been found that the glass transition behavior of POSS-containing hybrid material is decided by several factors. First, T_g of hybrid material is quite depended on both types of R groups around silsesquioxane cages and the interactions between R groups and polymer matrices [30]. POSS-containing hybrid material could display enhanced or reduced glass transition temperatures. For instance, a small amount of POSS loadings gave rise to the significant enhancement of T_g in cyclopentyl (and/or cyclohexyl) POSS styryl-co-4-methyl styrene copolymers [11,31]. Furthermore, the counterpart nanocomposites with cyclohexyl groups displayed the enhanced T_g in comparison with the cyclopentyl groups [32]. Second, T_g depression could be ascribed to the decrease of cross-linking density [33]. The last but not the least, it should be pointed out that in POSS-modified polymer systems, polymer will be reinforced by POSS because the POSS cages on polymer matrices could restrict the motions of polymer chains due to the tether structure. In the present case of pre-reacted system, the seven isobutyl groups of POSS molecule are mainly responsible for the depression of the glass transition because of the compatibility between isobutyl groups and epoxy matrix. Meanwhile, monofunctional AH-POSS reacted with some epoxy group, which will take up some cross-linking points, thus the cross-linking density will decrease. However, POSS cages were chemically bonded onto the cross-linking networks, which could contribute the inhabitation effect of POSS cages partly on the molecular motion. It is worth noticing that only while the AH-POSS content increased, the hybrid material displays the reduced T_g's. The fact that the glass transition temperatures of hybrid materials did not monotonously decrease with the increase of POSS concentration suggests that the change of T_g is affected by the above comprehensive embodiment of several factors. The decreased T_g's are also reported in several POSS-containing epoxy nanocomposites [34].

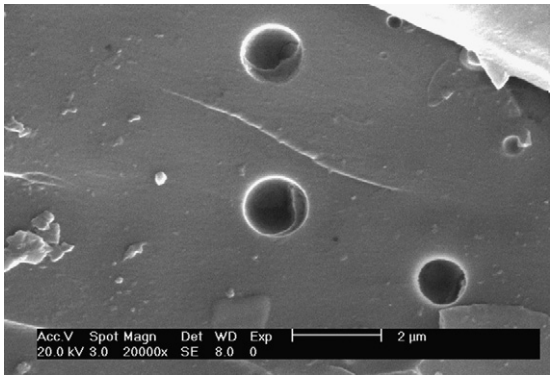

Fig. 6. SEM micrographs of non-reacted system hybrid material with 5 wt% AH-POSS.

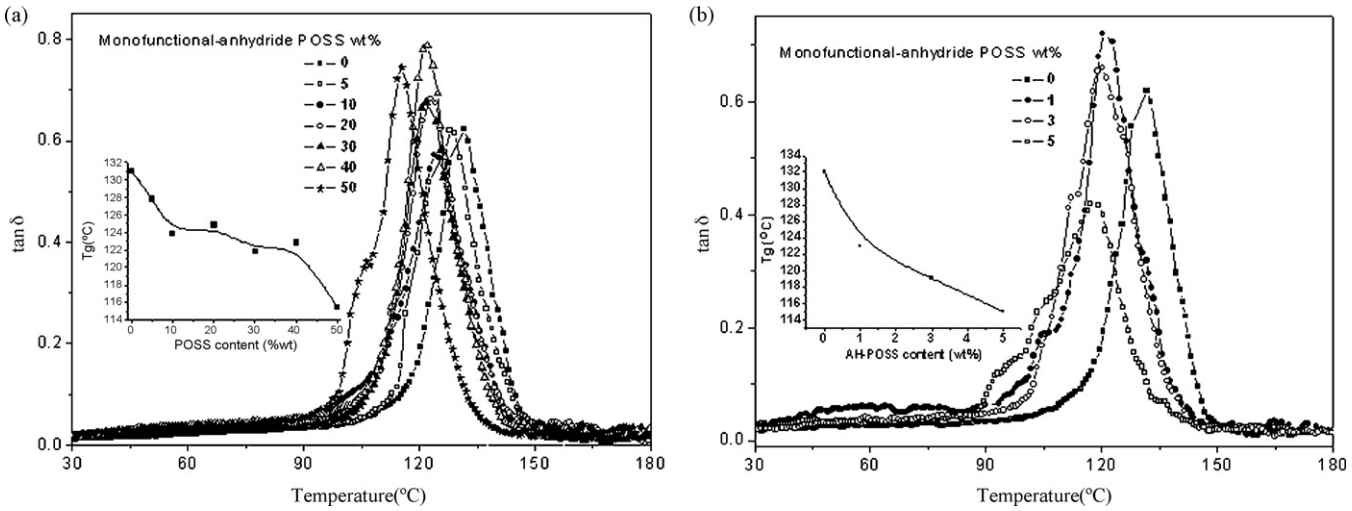

Fig. 7. The plots of DMA tan δ as functions of temperature for pre-reacted system (a) and non-reacted system (b) hybrid materials in the temperature range of 30–180 °C.

For non-reacted system (Fig. 7b), T_g of the hybrid material decreases with the increase of AH-POSS content. It has been proposed that the depression of T_g's could result from the phase separation due to the incompatibility between isobutyl groups and the epoxy matrix [35].

3.4.2. Dynamic mechanical properties

Curves of dynamic storage modulus are the plots of storage modulus (E', $E = E' + iE''$) as functions of temperature for the control epoxy and the hybrid materials with the AH-POSS content up to 40 wt% (Fig. 9a). Storage modulus indicates the storage of energy in samples under stress–strain. It is interesting to note that in the glass state and rubbery state, the dynamic storage modulus were significantly lower than that of the control epoxy with the increase of AH-POSS content except the modulus of the samples with 40 wt% AH-POSS. The modulus is irregularly increased while AH-POSS content is 40 wt%.

Because the curing reaction has been carried out to completion, the depression of E' would be ascribed to other reasons. As far as we known, the modulus of polymer networks is also generally related to the cross-linking density of the materials. It has also been proposed that the POSS–POSS interactions have a dominant role in controlling the resulting physical properties of modified system and the POSS–POSS interactions are important in the hybrid systems with chemically grafted POSS [36]. In addition, the nano-reinforcement of POSS cages would bring improvement for POSS/polymer hybrid materials. The incorporation of the compact POSS blocks in the cross-linking networks brings about reinforcement of local chains.

In the present case of pre-reacted system, POSS molecules were chemically bonded onto the epoxy chains and the POSS are the dangling units of the chain. POSS–POSS interactions formed POSS domains. The incompatibility of aliphatic R groups of isobutyl and epoxy matrix could contribute to the decrease in modulus for the hybrid materials [30]. When $T < T_g$, the molecular chain is frozen, and spherical cage type POSS can be used as "rolling ball" lubricant for the frozen chain, which will weaken the interaction between chains. As a result, the E' depressed with the increase of AH-POSS content. In rubbery state, the moduli of epoxy networks are generally related to cross-linking density. AH-POSS was tethered into the epoxy system and took up some cross-linking points. Thus, the cross-linking densities of materials are expected to be lower than that of the control epoxy. When AH-POSS content is lower than 30 wt%, polymerization-induced phase separation occurred and the cross-linking densities will decrease with the increase of POSS content in hybrid materials. So the depression of modulus has been

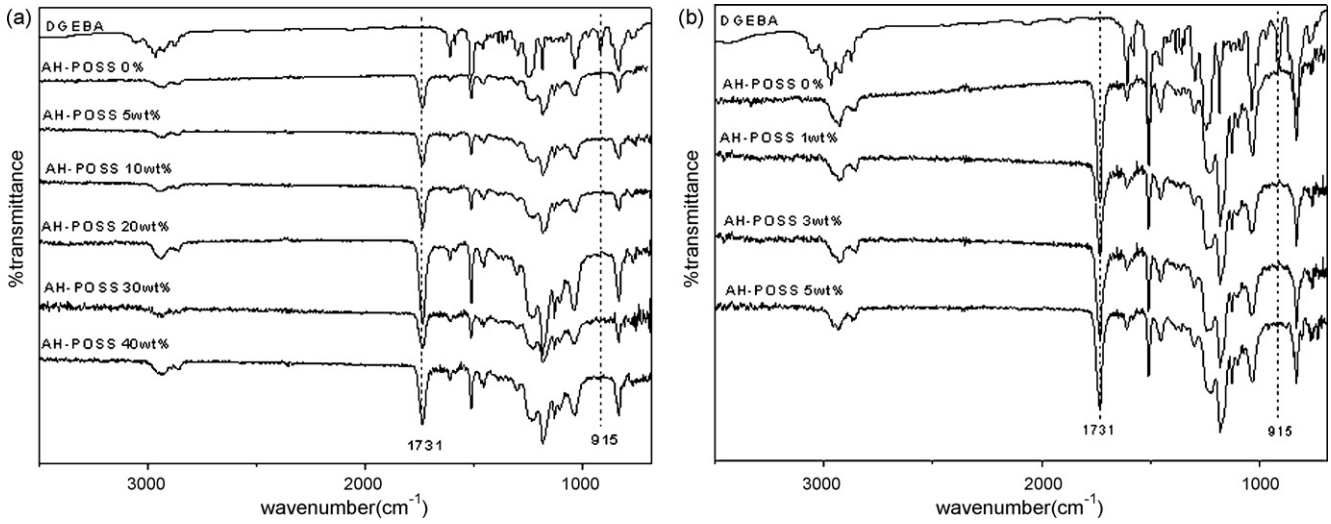

Fig. 8. FTIR spectra of the control epoxy and pre-reacted system (a) and non-reacted system (b) hybrid materials.

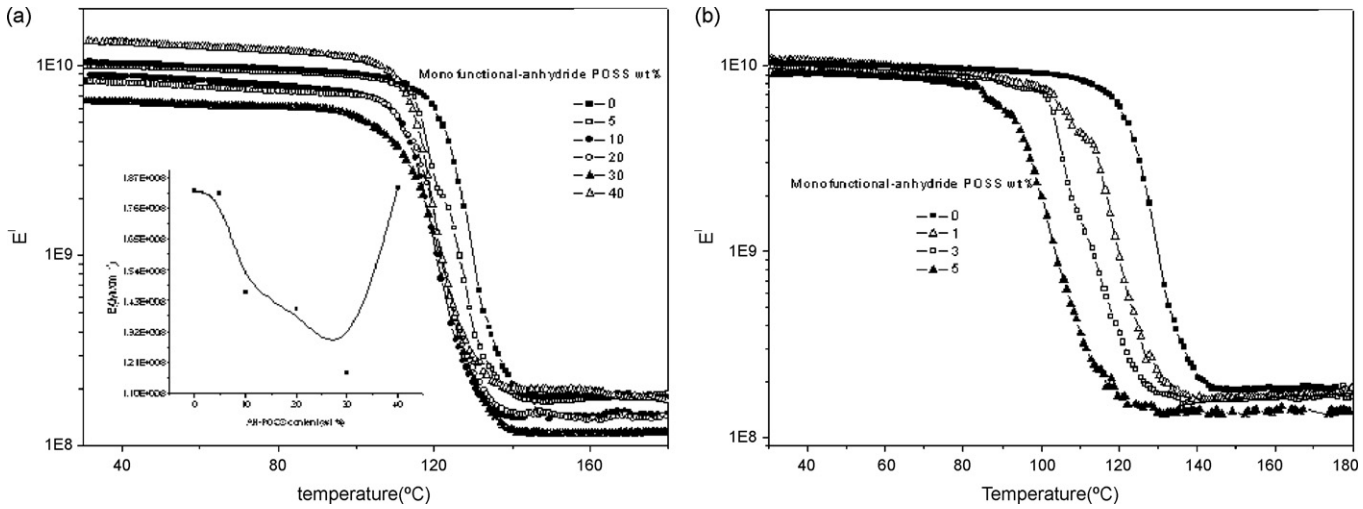

Fig. 9. The plots of DMA dynamic storage modulus as functions of temperature for pre-reacted system (a) and non-reacted system (b) hybrid materials.

decided mainly by the above factors. However, it is obvious that the modulus is irregularly increased and higher than others, when AH-POSS content is 40 wt%. In this sample, macro-phase separation occurred either before or after curing. Because the DGEBA is a selective solvent for AH-POSS-epoxy precursor, it could be assumed that POSS rich phase and DGEBA rich phase are formed before curing when the AH-POSS content is 40 wt%. After curing, the cross-linking density of DGEBA rich phase is improved because of its lower content of AH-POSS-epoxy precursor in the DGEBA rich phase. Moreover, with the nano-reinforcement of the POSS rich phase, the modulus is increased.

For non-reacted system (Fig. 9b), it is noted that the modulus of the hybrid material exhibited monotonous decrease as a function of POSS concentration. Phase separation and the incompatibility of the isobutyl groups of AH-POSS and the epoxy matrix mainly contribute to the decrease in modulus for hybrid material, especially at higher concentration of AH-POSS. Nonetheless, there is a significant difference in dynamic mechanic properties between pre-reacted and non-reacted system.

3.5. Thermal stability

The thermal stability of the composites was investigated with thermogravimetric analysis (TGA). Fig. 10 shows the TGA curves of the materials, recorded in an air atmosphere. The changes in thermal stability for epoxy networks by incorporating AH-POSS molecules into the systems were observed for the two systems in terms of both rates of weight loss from segmental decomposition and ceramic char. The initial thermal decomposition temperature (T_d) is defined as the temperature at which the mass loss of 5 wt% occurs.

For pre-reacted system, it is assumed that the covalent formed in AH-POSS-epoxy precursor chemically bonding into the network contributed to the enhancement of the initial decomposition temperature. In addition, it has been proposed that the tether structure was crucial to improvement in thermal stabilities of POSS-containing nanocomposites [17,37]. However, the decreased T_d for the composites could result from the increased chain spacing, which establishes more space for oxygen to enter. In the present case, POSS cages participated in the formation of the cross-linking network and in other words, the POSS cages were tethered into polymer matrix. Because of the relatively large volume comparing with the epoxy chain, the increased chain spaces were established with the AH-POSS incorporation. Thus, the initial T_d was decreased. However, it should be pointed out that the higher T_d for the phase-separated composite containing 40 wt% AH-POSS could be related the macro-phase separation and the T_d will be close to that of control epoxy. Also it is noted that the ceramic char of hybrid materials

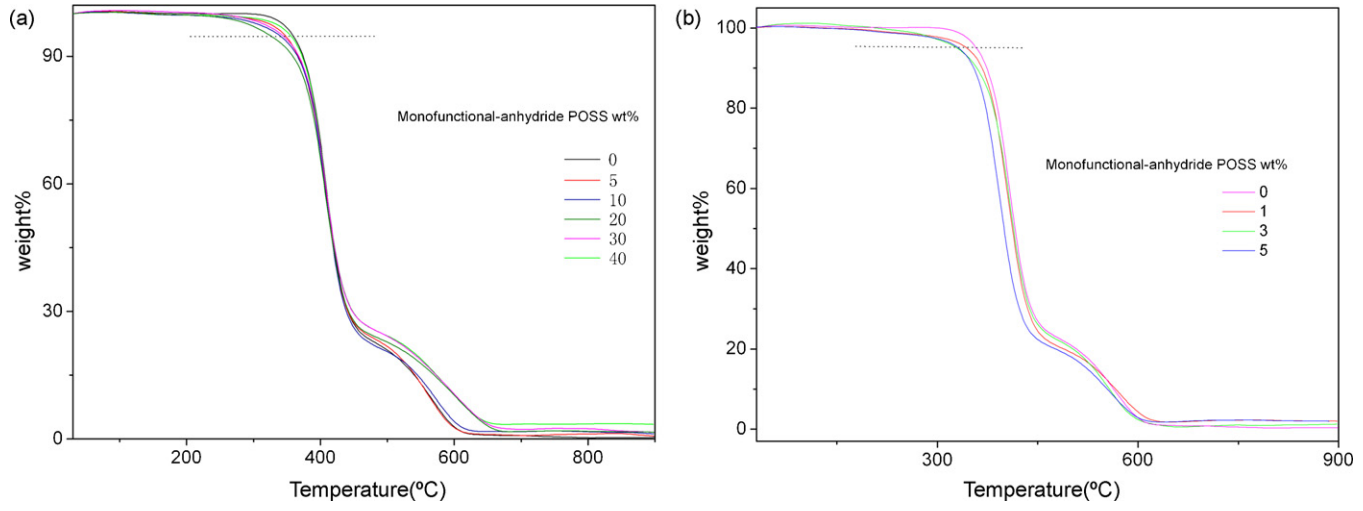

Fig. 10. TGA thermograms of pre-reacted (a) and non-reacted (b) hybrid materials.

are increased while the content of AH-POSS is higher. It is obvious to be seen that the more the content of AH-POSS is, the more stable the composite is at the higher temperature, which could be interpreted that POSS could form the SiO_2 layer to prevent decomposition of the hybrid material during the heating process, which indicates the good flame retardancy.

For non-reacted system, the reason for decrease of initial T_d is that phase separation happened. AH-POSS molecules in the dispersed phase could be converted into the silica particles via the condensation reaction among Si–O–Si at elevated temperatures. The silica particles are quite stable in the system until the mass loss from segmental decomposition of organic component undergo to completion. Therefore, the rates of mass loss from segmental decomposition were significantly decreased at higher temperature.

Within the test temperature range, all the TGA curves display two-step decomposition mechanism, Firstly organic part decomposed, then the Si–O–Si is transformed to SiO_2 [38]. It suggested that the existence of POSS did not significantly alter phase separation content results in a higher char, as would be expected.

4. Conclusions

AH-POSS was synthesized via the hydrosilylation reaction between THPA and $(i\text{-}C_4H_9)_7Si_8O_{12}OSi(CH_3)_2H$. Then AH-POSS was incorporated into DGEBA to prepare organic–inorganic hybrid materials with HHPA as curing agent. For the pre-reacted system, while the AH-POSS content is lower than 30 wt%, polymerization-induced phase separation occurred. When AH-POSS content is higher than 30 wt%, the macro-phase separation happened before and after curing. It is plausibly proposed that DGEBA has a certain solubility of AH-POSS-epoxy precursor.

For pre-reacted system, SEM and TEM micrograph indicates that the irregular clusters are formed with some nano "vesicle" structure inside and dispersed in the matrix with POSS content lower than 30 wt%. For non-reacted system, the spherical AH-POSS particles with diameter ranging from 1 to 2 μm are dispersed in the continuous epoxy matrices also with a few of irregular clusters.

The hybrid material with different microstructure displays different thermomechanical properties. For pre-reacted system, T_g's of hybrid materials are not monotonously decreased with the increase of AH-POSS content. The change in thermomechanical properties has been ascribed to the dispersion of AH-POSS-epoxy precursor, the formation of tether structure and the cross-linking density in the materials. The hybrid materials with POSS content lower than 30 wt% possess lower E's than that of control epoxy thermosets. But the E' of the sample with 40 wt% AH-POSS content is irregularly increased. The improvement of properties has been ascribed to the morphology and the compatibility of AH-POSS-epoxy precursor with epoxy matrix. The non-reacted system displayed the decreasing T_g's and storage modulus because of the prime macro-phase separation. In terms of thermogravimetric analysis, the pre-reacted system hybrid materials displayed the decreasing initial thermal decomposition temperatures (T_d's) with AH-POSS content lower than 30 wt%. However, when the AH-POSS content was up to 40 wt%, the T_d was closed to that of control epoxy. The non-reacted system hybrid material displayed the decreasing T_d's because of the initial phase separation and the incompatibility of isobutyl groups and the epoxy matrix.

Acknowledgments

This work was supported by the National Natural Science Foundation of China (50873082); Research Fund for the Doctoral Program of Higher Education (20070384047); Scientific and Technological Innovation Flat of Fujian Province (2009J1009).

Appendix A. Supplementary data

Supplementary data associated with this article can be found, in the online version, at doi:10.1016/j.matchemphys.2010.09.003.

References

[1] F.J. Feher, S.H. Phillips, J.W. Ziller, Journal of the American Chemical Society 119 (1997) 3397.
[2] C.X. Zhang, F. Babonneau, C. Bonhomme, R.M. Laine, C.L. Soles, H.A. Hristov, A.F. Yee, Journal of the American Chemical Society 120 (1998) 8380.
[3] C.X. Zhang, R.M. Laine, Journal of the American Chemical Society 122 (2000) 6979.
[4] R.M. Laine, J.W. Choi, I. Lee, Advanced Materials 13 (2001) 800.
[5] P.S.G. Krishnan, C.B. He, C.T.S. Shang, Journal of Polymer Science Part A: Polymer Chemistry 42 (2004) 4036.
[6] P.S.G. Krishnan, C.B. He, Journal of Polymer Science Part A: Polymer Chemistry 43 (2005) 2483.
[7] J.W. Choi, R. Tamaki, S.G. Kim, R.M. Laine, Chemistry of Materials 15 (2003) 3365.
[8] L.H. Lee, W.C. Chen, Polymer 46 (2005) 2163.
[9] Y.S. Lai, C.W. Tsai, H.W. Yang, G.P. Wang, K.H. Wu, Materials Chemistry and Physics 117 (2009) 91.
[10] H.U. Kim, Y.H. Bang, S.M. Choi, K.H. Yoon, Composites Science and Technology 68 (2008) 2739.
[11] A. Lee, J.D. Lichtenhan, Macromolecules 31 (1998) 4970.
[12] I.S. Isayeva, J.P. Kennedy, Journal of Polymer Science Part A: Polymer Chemistry 42 (2004) 4337.
[13] T. Gunji, Y. Iizuka, K. Arimitsu, Y. Abe, Journal of Polymer Science Part A: Polymer Chemistry 42 (2004) 3676.
[14] W.A. Wahab, I. Kim, C.S. Ha, Journal of Polymer Science Part A: Polymer Chemistry 42 (2004) 5189.
[15] G.Z. Li, H. Cho, L.C. Wang, H. Toghiani, C.U. Pittman, Journal of Polymer Science Part A: Polymer Chemistry 43 (2005) 355.
[16] K.W. Liang, H. Toghiani, G.Z. Li, C.U. Pittman, Journal of Polymer Science Part A: Polymer Chemistry 43 (2005) 3887.
[17] J. Choi, J. Harcup, A.F. Yee, Q. Zhu, R.M. Laine, Journal of the American Chemical Society 123 (2001) 11420.
[18] B.X. Fu, M. Namani, A. Lee, Polymer 44 (2003) 7739.
[19] G.M. Kim, H. Qin, X. Fang, F.C. Sun, P.T. Mather, Journal of Polymer Science Part B: Polymer Physics 41 (2003) 3299.
[20] T.L. Lu, G.Z. Liang, Y.L. Peng, T. Chen, Journal of Applied Polymer Science 106 (2007) 4117.
[21] H.Z. Liu, S.X. Zheng, K.M. Nie, Macromolecules 38 (2005) 5088.
[22] M.J. Abad, L. Barral, D.P. Fasce, R.J.J. Williams, Macromolecules 36 (2003) 3128.
[23] A. Strachota, I. Kroutilova, J. Kovarova, L. Matejka, Macromolecules 37 (2004) 9457.
[24] J. Choi, A.F. Yee, R.M. Laine, Macromolecules 37 (2004) 3267.
[25] Y.L. Liu, G.P. Chang, Journal of Polymer Science Part A: Polymer Chemistry 44 (2006) 1869.
[26] R. Duchateau, U. Cremer, R.J. Harmsen, S.I. Mohamud, H.C.L. Abbenhuis, R.A. van Santen, A. Meetsma, S.K.H. Thiele, M.F.H. van Tol, M. Kranenburg, Organometallics 18 (1999) 5447.
[27] E.G. Shockey, A.G. Bolf, P.F. Jones, J.J. Schwab, K.P. Chaffee, T.S. Haddad, J.D. Lichtenhan, Applied Organometallic Chemistry 13 (1999) 311.
[28] S. Wu, T. Hayakawa, R. Kikuchi, S.J. Grunzinger, M. Kakimoto, Macromolecules 40 (2007) 5698.
[29] I.A. Zucchi, M.J. Galante, R.J.J. Williams, E. Franchini, J. Galy, J.F. Gerard, Macromolecules 40 (2007) 1274.
[30] Y.H. Liu, S.X. Zheng, K.M. Nie, Polymer 46 (2005) 12016.
[31] P.T. Mather, H.G. Jeon, A. Romo-Uribe, T.S. Haddad, J.D. Lichtenhan, Macromolecules 32 (1999) 1194.
[32] A. Romo-Uribe, P.T. Mather, T.S. Haddad, J.D. Lichtenhan, Journal of Polymer Science Part B: Polymer Physics 36 (1998) 1857.
[33] G.Z. Li, L.C. Wang, H.L. Ni, C.U. Pittman, Journal of Inorganic and Organometallic Polymers 11 (2001) 123.
[34] Y. Ni, S.X. Zheng, K.M. Nie, Polymer 45 (2004) 5557.
[35] G.Z. Li, L.C. Wang, H. Toghiani, T.L. Daulton, K. Koyama, C.U. Pittman, Macromolecules 34 (2001) 8686.
[36] L. Matejka, A. Strachota, J. Plestil, P. Whelan, M. Steinhart, M. Slouf, Macromolecules 37 (2004) 9449.
[37] J. Fu, L.Y. Shi, Y. Chen, S. Yuan, J. Wu, X.L. Liang, Q.D. Zhong, Journal of Applied Polymer Science 109 (2008) 340.
[38] J. Choi, S.G. Kim, R.M. Laine, Macromolecules 37 (2004) 99.